Available online at www.sciencedirect.com
ScienceDirect
ELSEVIER
Polymer 48 (2007) 7065–7077
polymer
www.elsevier.com/locate/polymer

Poly(dibenzo[*a*,*c*]phenazine-2,7-diyl)s – Synthesis and characterisation of a new family of electron-accepting conjugated polymers

Julien E. Gautrot*, Philip Hodge*

Department of Chemistry, University of Manchester, Oxford Road, Manchester M13 9PL, UK

Received 4 June 2007; received in revised form 26 September 2007; accepted 28 September 2007
Available online 5 October 2007

Abstract

A new family of conjugated polymers containing dibenzo[*a*,*c*]phenazine moieties, and hence having moderately high electron affinities, has been synthesized. Syntheses were achieved using Yamamoto or Suzuki couplings with 2,7-dibromodibenzo[*a*,*c*]phenazine derivatives as monomers. Several of the polymers had significant molecular weights and were still soluble in tetrahydrofuran or chloroform. A series of model compounds were also synthesized to assist in characterizing the polymers. The UV–vis spectra of the various materials gave clear evidence of the existence of conjugation along the polymer backbones. Fluorescence measurements indicate that emission in the green to orange region, and possibly beyond, is sensitive to the 11- and 12-substituents on the dibenzophenazine moieties. Finally, cyclic voltammetry demonstrates the electron-accepting nature of these materials with electron affinities in the range 2.6–3.2 eV.
© 2007 Elsevier Ltd. All rights reserved.

Keywords: Conjugated polymers; Dibenzophenazine; Electron-accepting polymers

1. Introduction

The study of π-conjugated polymers is an ever-growing research field. One of the areas for which such materials show great promise is field effect transistors (FETs). Despite great advances in the general field of FETs, many problems still remain to be addressed. The physical processes underlying FET technologies are now well understood in the case of silicon and, more generally, inorganic semiconductors, but there still needs to be further studies of organic materials. One of the main differences characterizing organic semiconductors, as compared to their inorganic counterparts, is their relatively low level of order. As a consequence, charge mobilities within organic materials are considerably lower, indeed, typically by several orders of magnitude, when compared to silicon. In recent years various theories have been developed in an attempt to rationalize experimental observations and measurements [1]. Recently, Bredas and co-workers have stressed the importance of two different parameters in charge transport within ordered molecular materials [2]. First, the overlap integral characterizing the orbital overlap between two adjacent molecules (which influences intermolecular charge delocalisation) and, second, the reorganisation energy that is lost upon charge formation and that characterizes the relaxation of the molecule (hence influencing intramolecular charge delocalisation).

Much of the research effort that has been devoted to polymeric semiconductors has involved electron-rich systems possessing high ionisation potentials, for example, regioregular poly(3-hexylthiophene) and polyfluorene derivatives. Polythiophenes were found to possess the best characteristics for charge transport, for example high crystallinity, and to display the highest hole mobilities reported to date for a polymer [3]. There are, however, far fewer examples of high electron affinity conjugated polymers displaying useful electron mobilities, although recent studies suggest that the use of hydroxyl-group free gate dielectrics could allow the observation of high FET n-type mobility in many organic semiconductors [4]. Poly(oxobenzimidazoquinoline) is the only conjugated

---

* Corresponding authors.
E-mail addresses: jeg45@cam.ac.uk (J.E. Gautrot), philip.hodge@man.ac.uk (P. Hodge).

0032-3861/$ - see front matter © 2007 Elsevier Ltd. All rights reserved.
doi:10.1016/j.polymer.2007.09.045

polymer for which electron mobilities as high as 0.1 $cm^2 V^{-1} s^{-1}$ have been reported [5]. Recently, Bredas and co-workers published a theoretical study showing that phenazine-based discotic liquid crystalline molecules are expected to display remarkably small reorganisation energies upon reduction [2d,6]. Polymers based on derivatives of these materials could therefore possess improved electron transport properties as well as high electron affinities. In this paper we present the results of an exploratory study on the synthesis, solubility and photophysical and electrochemical properties of some novel polydibenzophenazines together with parallel studies on relevant model compounds.

Some polymers based on phenazine moieties linked via 2,7-linkages have already been reported in the literature, but they were found to be highly insoluble [7a–c]. Very recently, Jenekhe and co-workers reported the synthesis and photophysical properties of some soluble poly(dibenzo[*a*,*c*]phenazine-3,6-diyl)/dioctylfluorene) co-polymers [7d] (see Fig. 1 for numbering of the dibenzo[*a*,*c*]phenazine nucleus) and used them in blue-light-emitting diodes. Linking through the 3- and 6-positions is, however, not expected to give polymers with a π-electron system conjugated along the backbone. In the expectation of obtaining polymers with a more conjugated backbone, we chose 2,7-dibromodibenzo[*a*,*c*]phenazines as the core building block for a new family of electron-accepting conjugated polymers. The rationale behind this choice of approach is the following (Fig. 1): (i) a fully conjugated phenanthrene backbone allows intramolecular electron (and more generally energy) transfers to occur, (ii) the phenazine side chain moieties confer high electron affinities to the polymers, (iii) these moieties are expected to facilitate intermolecular electron transfers [2d,6], and (iv) various substituents attached to the 10- to 13-positions of the phenazine moiety may allow fine tuning of the solubility, thermotropic, photophysical and/or electrochemical properties of the materials.

2. Experimental section

2.1. General methods

All chemicals and solvents were purchased from Aldrich, Lancaster, Fluka, Avocado or Strem. Unless stated otherwise they were used without further purification. $Pd(PPh_3)_4$ [8a], 9,9-dioctylfluorene-2-boronic acid pinacol ester [8b], 9,9-dioctylfluorene-2,7-diboronic acid bispinacol ester [8b], 5,5′-bis(tri-*n*-butylstannyl)-2,2′-dithiophene [8c], 2,7-dibromophenanthraquinone (**2**) [8d], 1,2-dinitro-4,5-bismethoxybenzene [8e] and 1,2-dinitro-4,5-bisdodecyloxybenzene [8e] were synthesized as described in the literature.

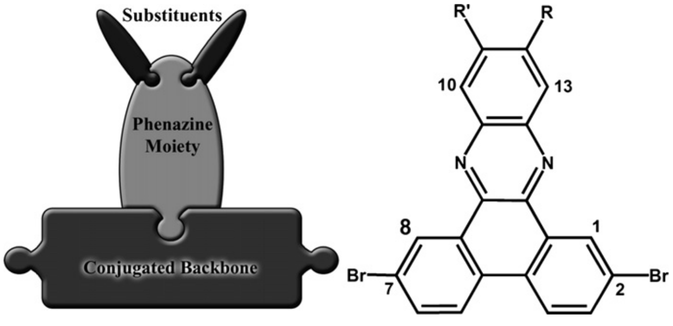

Fig. 1. Schematic of the design of polydibenzo[*a*,*c*]phenazines and typical molecular structure of a monomer.

Organic solutions were dried over magnesium sulfate. Purifications by flash column chromatography were achieved using Merck 9385 silica gel 60 (230–400 mesh). Thin layer chromatography (TLC) was carried out using Merck silica gel (60–254 mesh) coated on PET plates. Melting points were measured using a Gallenkamp melting point apparatus.

FT-IR spectra were recorded on a Perkin–Elmer spectrometer with an He/Ne 633 nm (<0.4 mW) laser. UV–vis spectra were recorded using a Unicam UV 300 spectrometer. Fluorescence spectroscopy was carried out using a Perkin–Elmer LS 55 spectrometer. Fluorescence quantum yields were measured using quinine sulfate in aqueous H_2SO_4 for the calibration [9]. Unless cited otherwise NMR spectra were recorded on a Varian Inova 300 MHz spectrometer for solutions in a mixture of $CDCl_3$ and trifluoroacetic acid (TFA) (95/5 v/v). TFA was necessary to increase the solubility of the compound. Mass spectrometry (MS) was carried out using a Micromass Trio 2000 instrument for EI/CI MS, a Micromass Platform instrument for electrospray MS and a Micromass TOF Spec 2E instrument for MALDI-TOF-MS. Size exclusion chromatography (SEC) was carried out using a three column system composed of two Polymer Labs Gel 30 cm 10 μm mixed B columns and one 500 Å column, a Knauer 64 pump (flow rate of 1 mL min^{-1}) and a Gilson 132 differential refractometer for the THF system. For the chloroform system, four Polymer Labs 3 μm mixed E columns, a Gilson 307 pump (flow rate 0.3 mL min^{-1}) and a GBC LC 1240 differential refractometer for detection were used. Both systems were calibrated with polystyrene standards. Elemental analyses were performed by the Microanalysis laboratory of the Department of Chemistry, University of Manchester. DSC measurements were carried out using a Seiko DSC 220G instrument (melting points – Mp – are defined as the trough's minimum). TGA measurements were carried out using a Seiko TG/DTA 220 instrument. Cyclic voltammograms (CVs) were recorded using a CH Instruments Electrochemical Workstation. The working electrode was glassy carbon, the counter electrode was a platinum wire and the reference electrode was Ag/AgCl (all measurements were carried out under argon atmosphere). In order to allow comparisons to be made between the different CV measurements, similar experimental conditions were used throughout this study. For the model compounds, CVs were recorded for solutions in dichloromethane (DCM), using tetra-*n*-butylammonium hexafluorophosphate ($TBAPF_6$) as the electrolyte. Unless otherwise stated CVs for polymers were recorded using thin films cast onto the carbon electrode, with tetraethylammonium hexafluorophosphate in acetonitrile as the electrolyte solution. Abbreviations used to describe various spectra and data: s, singlet; d, doublet; t, triplet; q, quartet; m, multiplet; br b, broad band; br p, broad peak; br s, broad singlet; br d, broad doublet; br m, broad multiplet; ib, intense band; obs, observed; req, required; sh, shoulder; wsh, weak shoulder.

2.2. Synthesis of materials

2.2.1. General procedure for the synthesis of dibenzo[a,c]phenazines **3**, **4**, **6** and **7**. 11-Methyldibenzo[a,c]phenazine (**3**)

9,10-Phenanthraquinone (**1**) (1.00 g, 4.81 mmol), toluene (50 mL) and 3,4-diaminotoluene (0.590 g, 4.81 mmol) were placed in a round-bottomed flask (1-neck, 100 mL) fitted with a condenser. The mixture was heated under reflux for 1 h and then allowed to cool to room temperature. Upon cooling, long thin needles crystallized. These were filtered off and washed with methanol (3 × 50 mL). Recrystallisation from toluene afforded colourless needles (0.93 g, 64%). Mp 219–220 °C (220 °C [10a]); IR (KBr, cm^{-1}) 3066, 2932, 1623 and 1606; ^1H NMR ($CDCl_3$, ppm) δ 9.33 (2H, d, $J = 7.3$ Hz), 8.50 (2H, d, $J = 7.8$ Hz), 8.16 (1H, d, $J = 8.7$ Hz), 8.04 (1H, s), 7.82–7.59 (5H, m) and 2.65 (3H, s, Me); ^{13}C NMR ($CDCl_3$, ppm) δ 22.21, 122.9, 126.1, 126.2, 127.9, 128.0, 129.0, 130.0, 130.2, 130.4, 131.8, 132.0, 132.5, 140.4, 140.8 and 142.2 (16 obs, 21 req); MS (EI/CI) 295 g mol^{-1}, $C_{21}H_{14}N_2H^+$ requires 295 g mol^{-1}.

2.2.2. Dibenzo[a,c]phenazine-11-carboxylic acid (**4**)

Yield 73%; Mp 316–318 °C (320 °C [10b]); IR (KBr, cm^{-1}) 2991 (br b), 2873, 2661, 1697 (ib) and 1605; ^1H NMR (ppm) δ 9.41 (1H, s), 9.35 (1H, d, $J = 8.1$ Hz), 9.22 (1H, d, $J = 8.2$ Hz), 8.86–8.67 (4H, m), 8.12 (2H, m) and 7.96 (2H, m); ^{13}C NMR (ppm) δ 124.3, 124.4, 125.0, 125.1, 127.1, 127.3, 130.3, 130.5, 130.9, 133.3, 134.5, 135.1, 135.5, 136.6, 138.2, 139.3, 143.7 and 169.9 (18 obs, 21 req); MS (MALDI) 322 g mol^{-1}, $C_{21}H_{10}O_2N_2H^+$ requires 323 g mol^{-1}.

2.2.3. 2,7-Dibromo-11-methyldibenzo[a,c]phenazine (**6**)

Yield 67%; Mp 299–300 °C; IR (KBr, cm^{-1}) 3077, 2944, 2910 and 1622; ^1H NMR (ppm) δ 9.04 (2H, s, H-1), 8.39 (1H, d, $J = 8.8$ Hz), 8.26 (1H, s, H-10), 8.18 (2H, d, $J = 8.6$ Hz), 8.07 (1H, d, $J = 8.8$ Hz), 7.82 (2H, d, $J = 8.8$ Hz) and 2.84 (3H, s, Me); ^{13}C NMR (ppm) δ 23.0, 124.4, 125.2, 125.4, 125.6, 126.4, 126.8, 128.9, 129.2, 130.1, 131.1, 135.6, 135.9, 136.3, 136.9, 137.8, 138.1 and 149.2 (18 obs, 21 req); MS (MALDI) triplet 451/453/455 g mol^{-1}, $C_{21}H_{12}N_2Br_2H^+$ requires triplet 451/453/455 g mol^{-1}; microanalysis: calc: C, 55.8%, H, 2.7%, N, 6.2%, Br, 35.3%; found: C, 55.3%, H, 2.7%, N, 6.2%, Br, 35.5%.

2.2.4. 2,7-Dibromodibenzo[a,c]phenazine-11-carboxylic acid (**7**)

Yield 52%; Mp > 350 °C; IR (KBr, cm^{-1}) 3073 (br b), 2985, 2829, 2655, 2523, 1689 (ib) and 1621; ^1H NMR (ppm) δ 9.53 (1H, d, $J = 2.0$ Hz), 9.49 (1H, d, $J = 1.6$ Hz, H-10), 9.40 (1H, d, $J = 1.9$ Hz), 8.92 (1H, dd, $J = 1.6$ and 9.0 Hz, H-4), 8.77 (1H, d, $J = 9.0$ Hz, H-3), 8.60 (1H, d, $J = 8.9$ Hz), 8.55 (1H, d, $J = 8.9$ Hz), 8.25 (1H, dd, $J = 1.8$ and 8.8 Hz) and 8.21 (1H, dd, $J = 2.0$ and 8.8 Hz); ^{13}C NMR (ppm) δ 123.9, 124.5, 125.3, 125.7, 125.9, 126.4, 126.8, 130.1, 130.2, 131.4, 131.5, 133.7, 134.3, 135.5, 135.7, 138.1, 138.2, 139.3, 139.6, 142.8 and 169.9 (21 obs, 21 req); MS (MALDI) triplet 479/481/483 g mol^{-1}, $C_{21}H_{10}O_2N_2Br_2H^+$ requires triplet 479/481/483 g mol^{-1}; microanalysis: calc: C, 52.3%, H, 2.1%, N, 5.8%, Br, 33.1%; found: C, 52.4%, H, 2.0%, N, 5.8%, Br, 33.4%.

2.2.5. General procedure for the synthesis of alkoxy-substituted dibenzo[a,c]phenazines **5**, **8** and **9**. 11,12-Didodecyloxydibenzo[a,c]phenazine (**5**)

1,2-Didodecyloxy-4,5-dinitrobenzene (2.00 g, 3.72 mmol), ethanol (50 mL) and palladium (10% on carbon, 0.5 g) were placed in a flask under hydrogen pressure (50 bar) for 12 h with vigorous stirring. The dinitro derivative slowly reacted and the diamino compound that formed was soluble in ethanol. The catalyst, however, remained in suspension. The mixture was filtered under nitrogen and dropped into a degassed (argon) solution of 9,10-phenanthraquinone (**1**) (0.390 g, 1.86 mmol) and toluene (100 mL) in a round-bottomed flask (1-neck, 250 mL). The mixture was stirred for 4 h at room temperature and darkened quickly. A brown precipitate formed slowly. It was filtered off and washed with methanol (3 × 50 mL). Purification using chromatography (silica, petroleum ether/toluene 90/10) and recrystallisation from a toluene/ethanol (1/1) mixture afforded yellow needles (0.67 g, 56%). Mp (DSC) 150 °C; IR (NaCl, cm^{-1}) 2914, 2847 and 1620; ^1H NMR ($CDCl_3$, ppm) δ 9.35 (2H, m), 8.58 (2H, m), 7.74 (4H, m), 7.53 (2H, s, H-10), 4.27 (4H, t, $J = 6.6$ Hz, H-1′), 1.99 (4H, t, $J = 6.5$ Hz, H-2′), 1.58 (4H, m), 1.50–1.19 (32H, m) and 0.88 (6H, t, $J = 6.4$ Hz, H-12′); ^{13}C NMR ($CDCl_3$, ppm) δ 14.4, 23.0, 26.4, 29.2, 29.6, 29.7, 29.9, 30.0, 30.1, 32.2, 69.6, 106.8, 123.1, 125.8, 128.0, 129.6, 130.5, 131.6, 140.0 and 153.8 (20 obs, 22 req); MS (MALDI) 650 g mol^{-1}, $C_{44}H_{60}O_2N_{24}H^+$ requires 650 g mol^{-1}; microanalysis: calc: C, 81.4%, H, 9.3%, N, 4.3%; found: C, 81.2%, H, 9.4%, N, 4.3%.

2.2.6. 2,7-Dibromo-11,12-dimethoxydibenzo[a,c]-phenazine (**8**)

Yield 22%; Mp 351–355 °C; IR (KBr, cm^{-1}) 3086, 2957, 2827 and 1621; ^1H NMR (ppm) δ 9.18 (2H, d, $J = 2.0$ Hz, H-1), 8.34 (2H, d, $J = 8.8$ Hz, H-4), 7.91 (2H, dd, $J = 2.0$ and 8.7 Hz, H-3), 7.80 (2H, s, H-10) and 4.26 (6H, s, Me); ^{13}C NMR (ppm) δ 57.9, 102.5, 124.3, 125.3, 125.7, 128.3, 130.0, 134.1, 135.6, 136.5 and 158.6 (11 obs, 11 req); MS (MALDI) triplet 495/497/499 g mol^{-1}, $C_{22}H_{14}O_2N_2Br_2H^+$ requires triplet 495/497/499 g mol^{-1}; microanalysis: calc: C, 53.0%, H, 2.8%, N, 5.6%, Br, 32.1%; found: C, 52.8%, H, 2.9%, N, 5.6%, Br, 32.2%.

2.2.7. 2,7-Dibromo-11,12-didodecyloxydibenzo[a,c]-phenazine (**9**)

Yield 19%; Mp 140–143 °C; IR (NaCl, cm^{-1}) 2920, 2850 and 1607; ^1H NMR ($CDCl_3$, ppm) δ 9.21 (2H, s, H-1), 8.17 (2H, d, $J = 8.8$ Hz, H-4), 7.71 (2H, d, $J = 8.6$ Hz, H-3), 7.34 (2H, s, H-10), 4.24 (4H, t, $J = 6.5$ Hz, H-1′), 2.00 (4H, m, H-2′), 1.59 (4H, m, H-3′), 1.52–1.18 (32H, m) and 0.88 (6H, m, H-12′); ^{13}C NMR ($CDCl_3$, ppm) δ 14.4, 23.0, 26.4, 29.2, 29.7, 29.8, 30.0, 30.1, 32.2, 69.6, 106.7, 122.6, 124.5, 128.3, 129.3, 132.1, 132.3, 138.5, 140.4 and 154.1 (20 obs, 22 req); MS (MALDI) triplet 806/808/810 g mol^{-1}, $C_{44}H_{58}O_2N_2Br_2H^+$ requires triplet 806/808/810 g mol^{-1}; microanalysis: calc: C, 65.5%, H, 7.3%, N, 3.5%, Br, 19.8%; found: C, 65.2%, H, 7.2%, N, 3.5%, Br, 19.6%.

*2.2.8. General procedure for the synthesis of aryl-substituted dibenzo[a,c]phenazines **10**–**13**. 2,7-Bis(9′,9′-dioctylfluoren-2′-yl)-11-methyldibenzo[a,c]phenazine (**10**)*

2,7-Dibromo-11-methyldibenzo[*a*,*c*]phenazine (**6**) (250 mg, 0.58 mmol), 9,9-dioctylfluorene 2-boronic acid pinacol ester (755 mg, 1.46 mmol) and palladium[0]tetrakis(triphenylphosphine) (34 mg, 29 μmol) were placed in a round-bottomed flask (3-neck, 50 mL), fitted with a condenser, under nitrogen. Tetrahydrofuran (THF) (20 mL, degassed with argon) and tetra-*n*-butylammonium hydroxide (1.0 M solution in methanol, 2 mL) were added via a septum. The mixture was heated to reflux overnight, cooled and poured onto aqueous hydrochloric acid (0.1 M, 200 mL). This aqueous phase was extracted with dichloromethane (2 × 50 mL), washed with water (3 × 50 mL), dried, filtered off and the solvent evaporated under vacuum. Purification using chromatography (silica, petroleum ether/toluene 90/10) and recrystallisation from a toluene/ethanol/ethyl acetate (4/5/1) mixture afforded yellow needles (409 mg, 66%). Mp (DSC) 68 °C; IR (NaCl, cm^{-1}) 3062, 3037, 2926, 2853 and 1612; ^{1}H NMR ($CDCl_3$, ppm) δ 9.71 (2H, m), 8.67 (2H, d, $J = 8.5$ Hz), 8.29 (1H, d, $J = 8.7$ Hz), 8.18 (1H, s, H-10), 8.12 (2H, dd, $J = 2.1$ and 8.3 Hz), 7.95–7.83 (6H, m), 7.79 (2H, d, $J = 7.1$ Hz), 7.72 (1H, dd, $J = 1.7$ and 8.7 Hz), 7.44–7.31 (6H, m), 2.71 (3H, s, Me), 2.09 (8H, m, H-1″), 1.31–0.98 (40H, m) and 0.79 (20H, m, H-2″ and 8″); ^{13}C NMR ($CDCl_3$, ppm) δ 14.4, 22.4, 22.9, 24.2, 29.6, 30.4, 32.1, 40.7, 55.6, 120.2, 120.4, 122.0, 123.2, 123.8, 124.4, 124.6, 126.7, 127.1, 127.4, 128.4, 129.3, 129.4, 130.8, 130.9, 131.0, 132.7, 139.7, 139.8, 140.7, 141.0, 141.1, 141.2, 141.3, 142.2, 142.5, 142.8, 151.4 and 151.9 (38 obs, 63 req); MS (MALDI) 1072 g mol^{-1}, $C_{79}H_{94}N_2H^+$ requires 1072 g mol^{-1}; microanalysis: calc: C, 88.5%, H, 8.9%, N, 2.6%; found: C, 88.6%, H, 9.1%, N, 2.6%.

*2.2.9. 2,7-Bis(9′,9′-dioctylfluoren-2′-yl)dibenzo[a,c]-phenazine-11-carboxylic acid (**11**)*

Yield 67%; Mp (DSC) 64 °C; IR (NaCl, cm^{-1}) 3064 (br b), 3014, 2926, 2853, 2661, 1695 (ib) and 1618; ^{1}H NMR ($CDCl_3$, ppm) δ 9.46 (1H, s), 9.39 (1H, s), 8.99 (1H, s), 8.49–8.20 (4H, m), 8.04–7.61 (10H, m), 7.42 (6H, m), 2.15 (8H, m, H-1″), 1.32–0.98 (40H, m) and 0.96–0.66 (20H, m, H-2″ and 8″); ^{13}C NMR ($CDCl_3$, ppm) δ 14.3, 22.9, 24.3, 29.6, 30.4, 32.1, 40.7, 55.6, 120.3, 120.6, 121.8, 123.3, 123.6, 124.6, 124.9, 126.7, 127.2, 127.5, 129.2, 130.1, 130.8, 131.3, 133.7, 139.3, 141.0, 141.1, 141.2, 141.3, 143.7, 144.3, 151.5, 151.9 and 171.6 (33 obs, 63 req); MS (MALDI) 1102 g mol^{-1}, $C_{79}H_{92}O_2N_2H^+$ requires 1102 g mol^{-1}; microanalysis: calc: C, 86.1%, H, 8.4%, N, 2.5%; found: C, 86.1%, H, 8.1%, N, 2.3%.

*2.2.10. 2,7-Bis(9′,9′-dioctylfluoren-2′-yl)-11,12-dimethoxydibenzo[a,c]phenazine (**12**)*

Yield 68%; Mp (DSC) 104 °C; IR (NaCl, cm^{-1}) 3064, 3002, 2926, 2853 and 1612; ^{1}H NMR ($CDCl_3$, ppm) δ 9.68 (2H, d, $J = 1.9$ Hz, H-1), 8.69 (2H, d, $J = 8.6$ Hz, H-4), 8.11 (2H, dd, $J = 1.9$ and 8.4 Hz, H-3), 7.99–7.75 (8H, m), 7.60 (2H, s, H-10), 7.45–7.30 (6H, m), 4.15 (6H, s, Me), 2.10 (8H, m, H-1″), 1.27–1.00 (40H, m) and 0.84–0.67 (20H, m, H-2″ and 8″); ^{13}C NMR ($CDCl_3$, ppm) δ 14.3, 22.9, 29.5, 30.4, 32.1, 40.7, 55.6, 56.8, 106.3, 120.1, 120.4, 122.0, 123.2, 123.8, 124.0, 126.7, 127.1, 127.4, 128.5, 129.0, 129.3, 130.5, 139.8, 140.4, 141.1, 141.2, 151.4, 151.9 and 153.9 (29 obs, 32 req); MS (MALDI) 1119 g mol^{-1}, $C_{80}H_{96}O_2N_2H^+$ requires 1118 g mol^{-1}; microanalysis: calc: C, 86.0%, H, 8.7%, N, 2.5%; found: C, 86.0%, H, 8.7%, N, 2.5%.

*2.2.11. 2,7-Bis(thien-2′-yl)-11-methyldibenzo[a,c]-phenazine (**13**)*

Yield 98%; T_{dec} 325 °C; IR (KBr, cm^{-1}) 3064, 2953, 2868 and 1610; ^{1}H NMR (ppm) δ 8.90 (2H, br p), 8.27 (1H, br p), 8.13 (1H, br p), 8.00 (2H, br p), 7.84 (1H, br p), 7.64 (2H, br p), 7.41 (3H, br m), 7.13 (2H, br d, $J = 7.8$ Hz), 7.00 (1H, br s) and 2.62 (3H, s, Me); ^{13}C NMR (ppm) δ 30.5, 121.7, 122.6, 124.3, 124.5, 125.3, 125.4, 125.8, 126.1, 128.8, 130.1, 130.7, 135.3, 135.5, 136.2, 137.3 and 141.5 (17 obs, 29 req); MS (MALDI) 459 g mol^{-1}, $C_{29}H_{18}N_2S_2H^+$ requires 459 g mol^{-1}.

*2.2.12. 2,7-Bis(5′-bromothien-2′-yl)-11-methyldibenzo-[a,c]phenazine (**14**)*

2,7-Bis(thien-2′-yl)-11-methyldibenzo[*a*,*c*]phenazine (**13**) (284 mg, 0.62 mmol), chloroform (50 mL) and trifluoroacetic acid (0.30 mL) were placed in a round-bottomed flask (1-neck, 100 mL). Bromine (208 mg, 1.30 mmol) was added dropwise. The reaction mixture was left to stir for 12 h at room temperature. It was then extracted with a sodium thiosulfate aqueous solution (0.1 M, 2 × 100 mL) and water (3 × 50 mL), dried, filtered and the solvent evaporated off under vacuum. Recrystallisation of the residue from *o*-xylene afforded yellow crystals (339 mg, 89%). T_{dec} 330 °C; IR (KBr, cm^{-1}) 3025, 2918, 2857 and 1609; ^{1}H NMR (ppm) δ 8.83 (2H, dd, $J = 1.8$ and 6.1 Hz), 8.28 (1H, d, $J = 8.8$ Hz, H-12), 8.13 (1H, s, H-10), 8.05–7.90 (3H, m), 7.58 (2H, m), 7.15 (2H, m), 7.05 (2H, m) and 2.72 (3H, s, Me); ^{13}C NMR (ppm) δ 22.9, 121.9, 122.9, 124.8, 125.2, 125.5, 125.6, 126.3, 129.8, 130.4, 131.5, 131.9, 134.6, 135.1, 137.0, 137.4, 143.1 and 148.7 (18 obs, 29 req); MS (MALDI) triplet 615/617/619 g mol^{-1}, $C_{29}H_{16}N_2S_2Br_2H^+$ requires triplet 615/617/619 g mol^{-1}.

*2.2.13. General procedure for the synthesis of polymers **15**–**21** using 2,7-dibromodibenzo[a,c]phenazine and Suzuki coupling. Poly(11,12-didodecyloxydibenzo-[a,c]phenazine-2,7-diyl-alt-benzen-1′,4′-diyl) (**15**)*

2,7-Dibromo-11,12-didodecyloxydibenzo[*a*,*c*]phenazine (**9**) (250 mg, 0.31 mmol), benzene-1,4-diboronic acid bispinacol ester (102 mg, 0.31 mmol) and palladium[0]tetrakis(triphenylphosphine) (18 mg, 16 μmol) were placed in a round-bottomed flask (3-neck, 50 mL), fitted with a condenser, under nitrogen. THF (10 mL, degassed with argon) and tetra-*n*-butylammonium hydroxide (1.0 M solution in methanol, 1 mL) were added via a septum. The mixture was heated under reflux overnight and poured onto aqueous hydrochloric acid (0.1 M, 200 mL) and methanol (200 mL), filtered off and washed with methanol. The yellow solid remaining was dissolved in a chloroform/TFA 9/1 mixture (30 mL), passed through a Hyflo plug, precipitated in a methanol/water 2/1 mixture (500 mL), filtered off and washed with methanol (3 × 50 mL). Purification of the yellow powder remaining was carried out by Soxhlet extraction using methanol for 72 h. Drying under vacuum for 48 h afforded a yellow solid (222 mg, 99%). DSC: no thermal transition could be observed between 25 °C and 250 °C; TGA: T_{dec}, 380 °C; IR (KBr, cm^{-1}) 2922, 2851 and 1619; ^{1}H NMR (ppm) δ 9.15–5.36 (12H, br m), 4.34 (4H, br p, H-1′) and 2.57–0.00 (46H, br m); ^{13}C NMR (ppm) δ 14.0, 22.8, 26.1, 28.8, 29.6, 30.5, 31.2, 32.3, 71.2, 124.0, 127.3, 127.8, 128.2, 129.4, 130.2 and 140.9 (16 obs, 24 req).

*2.2.14. Poly(11,12-didodecyloxydibenzo[a,c]phenazine-2,7-diyl-alt-biphen-4′,4″-diyl) (**16**)*

Yield 55%; DSC: no thermal transition could be observed between 25 °C and 250 °C; TGA: T_{dec}, 317 °C; IR (NaCl, cm^{-1}) 2923, 2853 and 1620; ^{1}H NMR (ppm) δ 8.61–7.38 (16H, br m), 3.81 (4H, br p, H-1′) and 2.33–0.48 (46H, br m); ^{13}C NMR (ppm) δ 14.3, 22.9, 26.1, 26.2, 29.6, 29.9, 32.2, 71.0, 123.8, 127.3, 127.7, 128.0, 129.2, 130.6, 154.9 and 157.6 (16 obs, 26 req); SEC ($CHCl_3$, g mol^{-1}) M_n 24,700, M_w 32,200.

*2.2.15. Poly(11-methyldibenzo[a,c]phenazine-2,7-diyl-alt-9′,9′-dioctylfluorene-2′,7′-diyl) (**17**)*

Yield 65%; DSC: no thermal transition could be observed between −50 °C and 240 °C; TGA: T_{dec}, 336.7 °C; IR (NaCl, cm^{-1}) 3058, 2924, 2851 and 1625; ^{1}H NMR (ppm) δ 9.56 (1H, br d), 8.86 (1H, br p), 8.60 (1H, br p), 8.45 (3H, br m), 8.21–7.59 (9H, br m), 2.86 (3H, br p, Me), 2.21 (4H, br m, H-1″), 1.18 (20H, br m) and 0.99–0.59 (10H, br m, H-2″ and 8″); ^{13}C NMR (ppm) δ 13.8, 22.5, 22.7, 24.1, 28.8, 29.4, 30.2, 31.9, 40.6, 55.8, 120.8, 121.2, 121.9, 124.4, 124.9, 126.5, 127.4, 129.0, 129.8, 133.0, 133.7, 138.1, 141.5, 143.3 and 152.7 (25 obs, 42 req); SEC (THF, g mol^{-1}) M_n 3800, M_w 8200.

*2.2.16. Poly(11-carboxy-dibenzo[a,c]phenazine-2,7-diyl-alt-9′,9′-dioctylfluorene-2′,7′-diyl) (**18**)*

Yield 93%; DSC: no thermal transition could be observed between −25 °C and 250 °C; TGA: T_{dec}, 325.5 °C; IR (NaCl, cm^{-1}) 3435 (br b), 3177, 2922, 2852, 2616, 1700 (ib) and 1609; ^{1}H NMR (ppm) δ 9.81–9.40 (2H, br m), 8.86 (4H, br m), 8.50 (1H, br p), 8.18–7.54 (8H, br m), 2.26 (4H, br p, H-1″), 1.33–1.01 (20H, br m) and 0.99–0.62 (10H, br m, H-2″ and 8″); ^{13}C NMR (ppm) δ 13.8, 22.6, 24.0, 29.3, 30.1, 31.9, 40.5, 56.0, 121.4, 121.7, 125.4, 126.6, 129.0, 133.9, 134.5, 137.8, 141.7, 143.8, 152.7 and 169.9 (20 obs, 42 req); SEC (THF, g mol^{-1}) M_n 2400, M_w 3500.

*2.2.17. Poly(11,12-dimethoxydibenzo[a,c]phenazine-2,7-diyl-alt-9′,9′-dioctylfluorene-2′,7′-diyl) (**19**)*

Yield 91%; DSC: no thermal transition could be observed between 25 °C and 350 °C; TGA: T_{dec}, 406.4 °C; IR (NaCl, cm^{-1}) 3004, 2923, 2850 and 1611; ^{1}H NMR (ppm) δ 9.53 (2H, br p), 8.85 (2H, br p), 8.37 (2H, br p), 8.02 (2H, br p), 7.95–7.61 (6H, br m), 4.25 (6H, br p, Me), 2.25 (4H, br p, H-1″), 1.33–1.00 (20H, br m) and 0.99–0.52 (10H, br m, H-2″ and 8″); ^{13}C NMR (ppm) δ 13.7, 13.9, 22.5, 23.9, 29.2, 31.7, 40.3, 57.4, 89.2, 95.7, 122.6, 124.4, 131.1, 139.3, 147.4, 152.4 and 157.4 (17 obs, 26 req); SEC ($CHCl_3$, g mol^{-1}) M_n 5500, M_w 10,900.

*2.2.18. Polymer (**20**)*

Yield 88%; DSC: no thermal transition could be observed between −25 °C and 350 °C; TGA: T_{dec}, 415.3 °C; IR (KBr, cm^{-1}) 2925, 2857 and 1609; ^{1}H NMR (ppm) δ 9.40–8.94 (2H, br m), 8.60–8.07 (4H, br m), 8.05–7.07 (13H, br m), 2.64 (3H, br p, Me), 2.16 (4H, br p, H-1″), 1.41–1.07 (20H, br m) and 1.00–0.60 (10H, br m, H-2″ and 8″); ^{13}C NMR (ppm) δ 13.6, 19.8, 22.4, 23.8, 29.2, 30.0, 31.7, 40.4, 55.4, 119.9, 124.5, 125.1, 126.0, 127.0, 128.5, 130.3, 137.1 and 151.0.

*2.2.19. Poly(11,12-didodecyloxydibenzo[a,c]phenazine-2,7-diyl-alt-2′,2″-dithien-5′,5″-diyl) (**21**)*

2,7-Dibromo-11,12-didodecyloxydibenzo[*a*,*c*]phenazine (**9**) (250 mg, 0.31 mmol) and palladium(0)tetrakis(triphenylphosphine) (18 mg, 16 μmol) were placed in a round-bottomed flask (3-neck, 50 mL), fitted with a condenser, under nitrogen. THF (10 mL, degassed with argon) and 5,5′-bis(tri-*n*-butylstannyl)-2,2′-dithiophene (276 mg, 0.37 mmol) were added via a septum. The mixture was heated under reflux overnight and poured into aqueous hydrochloric acid (0.1 M, 200 mL) and methanol (200 mL), filtered off and washed with methanol. The orange solid remaining was dissolved in THF (30 mL), passed through a silica plug, precipitated in water (500 mL), filtered off and washed with methanol (3 × 50 mL). Purification of the remaining orange powder was carried out by Soxhlet extraction using methanol for three days. Drying under vacuum for two days afforded an orange solid (186 mg, 74%). DSC: no thermal transition could be observed between 25 °C and 250 °C; TGA: T_{dec}, 340 °C; IR (NaCl, cm^{-1}) 2922, 2852, 1620 and 1608; ^{1}H NMR (ppm) δ 9.25–6.35 (12H, br m), 4.09 (4H, br p, H-1‴), 1.98 (4H, br p, H-2‴), 1.69–1.08 (36H, br m) and 1.02–0.69 (6H, br m, H-12‴); ^{13}C NMR (ppm) δ 13.9, 22.7, 25.9, 28.5, 28.6, 28.7, 29.4, 29.7, 31.9, 70.7, 71.2, 98.6, 120.7, 123.7, 125.4, 127.1, 128.0, 128.7, 130.0, 133.8, 134.2, 136.2, 138.4, 139.3, 156.4 and 158.9 (26 obs, 26 req); SEC ($CHCl_3$, g mol^{-1}) M_n 18,800, M_w 26,600.

*2.2.20. Synthesis of polymers **22** and **23** by Yamamoto coupling. Poly(11-methyldibenzo[a,c]phenazine-2,7-diyl) (**22**)*

2,7-Dibromo-11-methyldibenzo[*a*,*c*]phenazine (**6**) (400 mg, 0.94 mmol), bistriphenylphosphinenickel(II) chloride (65 mg, 0.10 μmol, anhydrous), zinc (195 mg, 3.00 mmol) and tetraethylammonium iodide (257 mg, 1.00 mmol) were placed in a flame-dried flask (2-neck, 50 mL) using a glove box. THF (10 mL, anhydrous) was added to the mixture via a septum. The green mixture was then heated to 80 °C: it turned red-brown. The mixture was left to stir for 3 h. It solidified. After being cooled to room temperature, the mixture was treated with crushed ice and dilute hydrochloric acid. The yellow solid obtained was filtered off, washed with methanol (3 × 50 mL) and dried in air. The yellow powder remaining was dissolved in a chloroform/TFA mixture (20/1) (30 mL). This solution was passed through a Hyflo plug, precipitated in methanol/water 2/1 (500 mL), the solid filtered off and washed with methanol (3 × 50 mL). Soxhlet extraction with methanol for three days and drying in vacuum for two days afforded a yellow solid (206 mg, 75%). DSC: no thermal transition could be observed between −50 °C and 200 °C; TGA: T_{dec}, 313 °C; IR (KBr, cm^{-1}) 3069, 2913 and 1622, ^{1}H NMR (ppm) δ 9.38 (1H, m), 8.99–8.70 (1H, m), 8.69–8.47 (3H, m), 8.38 (1H, m), 8.29–8.04 (2H, m), 7.98–7.46 (1H, m) and 2.86 (3H, m); ^{13}C NMR (ppm) δ 22.2, 22.5, 122.5, 124.6, 124.9, 125.0, 125.6, 125.7, 125.8, 126.3, 126.4, 129.1, 129.5, 130.9, 132.0, 137.0, 137.7, 138.2 and 150.0 (19 obs, 21 req).

2.2.21. *Poly(11,12-didodecyloxydibenzo[a,c]phenazine-2,7-diyl) (**23**)*

2,7-Dibromo-11,12-didodecyloxy-dibenzo[*a*,*c*]phenazine (**9**) (250 mg, 0.36 mmol), nickel bis(1,5-cyclooctadiene) (127 mg, 0.46 mmol, anhydrous) and 2,2′-bipyridine (72 mg, 0.46 mmol) were placed in a flame-dried round-bottomed flask (1-neck, 50 mL), fitted with a septum, in a glove box. Three cycles of vacuum and nitrogen were carried out before adding *N*,*N*-dimethylformamide (3 mL, anhydrous), toluene (10 mL, anhydrous) and 1,5-cyclooctadiene (127 mg, 0.46 mmol, anhydrous). The resulting mixture was degassed by operating three cycles of freeze–dry–thaw. The orange mixture was then heated up to 60 °C: it turned red-brown. The mixture was left to stir for 48 h by which time a solid had formed. The reaction mixture was poured into aqueous hydrochloric acid (0.1 M, 200 mL) and methanol (200 mL), filtered off and washed with methanol. The yellow solid remaining was dissolved in THF (30 mL), passed through a silica plug, precipitated in water (500 mL), filtered off and washed with methanol (3 × 50 mL). Purification of the yellow powder remaining was carried out by Soxhlet extraction using methanol for 72 h. Drying in vacuum for 48 h afforded a yellow solid (231 mg, 99%). DSC: no thermal transition could be observed between 25 °C and 250 °C; TGA: T_{dec}, 348 °C; IR (NaCl, cm^{-1}) 2923, 2853 and 1619; ^{1}H NMR (ppm) δ 10.25–6.49 (8H, br m), 5.09 (4H, br p, H-1′) and 2.59–0.31 (46H, br m); ^{13}C NMR (ppm) δ 14.1, 22.9, 26.1, 28.9, 29.3, 29.7, 30.0, 30.3, 32.2, 71.4, 125.0, 125.2, 125.4, 131.2, 131.3, 131.4, 131.5, 131.6, 157.7, 158.0 and 158.2 (21 obs, 22 req); SEC ($\mathrm{CHCl_3}$, g mol^{-1}) M_{n} 36,400, M_{w} 68,800.

3. Results and discussion

3.1. *Synthesis of materials and structural characterisation*

In the present work the required dibenzo[*a*,*c*]phenazine compounds were prepared by condensing phenanthrene-9,10-quinone (**1**) or 2,7-dibromophenanthrene-9,10-quinone (**2**) with the appropriate 1,2-diaminobenzene derivative. In this way the simple model dibenzophenazines **3–5** were prepared from quinone **1** and the dibromodibenzophenazine monomers **6–9** were prepared from quinone **2** (Scheme 1). The condensation reactions proceeded in good yields (50–75%) in the case of diamines bearing no strong electron-donor substituents, but in the case of the more electron-rich diamines (alkoxy derivatives) the stability of the diamino compound was so low that, to obtain useful quantities of the phenazines, the dialkoxydiamines had to be used immediately after preparation and oxygen had to be carefully excluded from the reaction mixture. Even then, the yields were only poor to modest. Competition with electron transfer reactions from the highly electron-rich diamine to the electron-acceptor phenanthraquinone is likely to be responsible for these low yields.

To assist in characterizing the polymers, the more complex model compounds **10–13** were prepared by Suzuki couplings between quinones **6–8** and either 9,9-dioctylfluorene-2-boronic acid pinacol ester or thiophen-2-boronic acid (Scheme 1). In order to improve the solubility of the starting materials in the reaction mixture, tetra-*n*-butylammonium hydroxide (which is soluble in THF) was used as a base instead of aqueous potassium carbonate. These reactions proceeded smoothly and in good yields (60–98%). Finally, a further dibromo monomer, compound **14**, was prepared by brominating thiophene-containing compound **13**.

Polymers **15–20** were prepared similarly by Suzuki couplings using appropriate dibromodibenzophenazine derivatives and diboronic acid esters (Scheme 2). For phenazines with small substituents, i.e. methyl, carboxylic acid and methoxy functional groups, 9,9-dioctylfluorene-2,7-diboronic acid dipinacol ester was used as the co-monomer to enhance the solubilities of the final polymers. Despite this, relatively short polymer chains were obtained, with M_{n}, by SEC analyses, ranging from 2400 to 5500 (Table 1) for polymers **17–19**. Polymer **20** was too insoluble for SEC analysis. With the didodecyloxy-substituted monomer **5**, the use of benzene-1,4-boronic acid dipinacol ester or biphenyl-4,4′-diboronic acid dipinacol ester as co-monomer afforded polymers **15** and **16**, respectively. The former was only soluble in chloroform/TFA mixtures but the latter was soluble in chloroform and THF. Polymer **16** had M_{n} of 24,700 (Table 1). A Stille coupling between dibromo compound **9** and 5,5′-bis(tributylstannyl)bithienyl afforded polymer **21** (Scheme 2). This had good solubility and M_{n} of 18,800: see Table 1.

Finally polymerisations to afford homopolymers **22** and **23** were carried out using Yamamoto couplings (Scheme 3). Using dibromo monomer **6** and an $\mathrm{NiCl_2/Zn}$ catalyst system only oligomers **22** were produced. These were insoluble in THF and chloroform but were soluble in chloroform/TFA (95:5 v/v) mixtures. This precluded SEC analysis. Monomer **9**, with two dodecyloxy substituents, was better suited to producing soluble polymer but the same polymerisation conditions only afforded oligomers **23** as evidenced by SEC and MALDI-TOF measurements. This is thought to be due to the low solubility of both monomer **9** and polymer **23** in

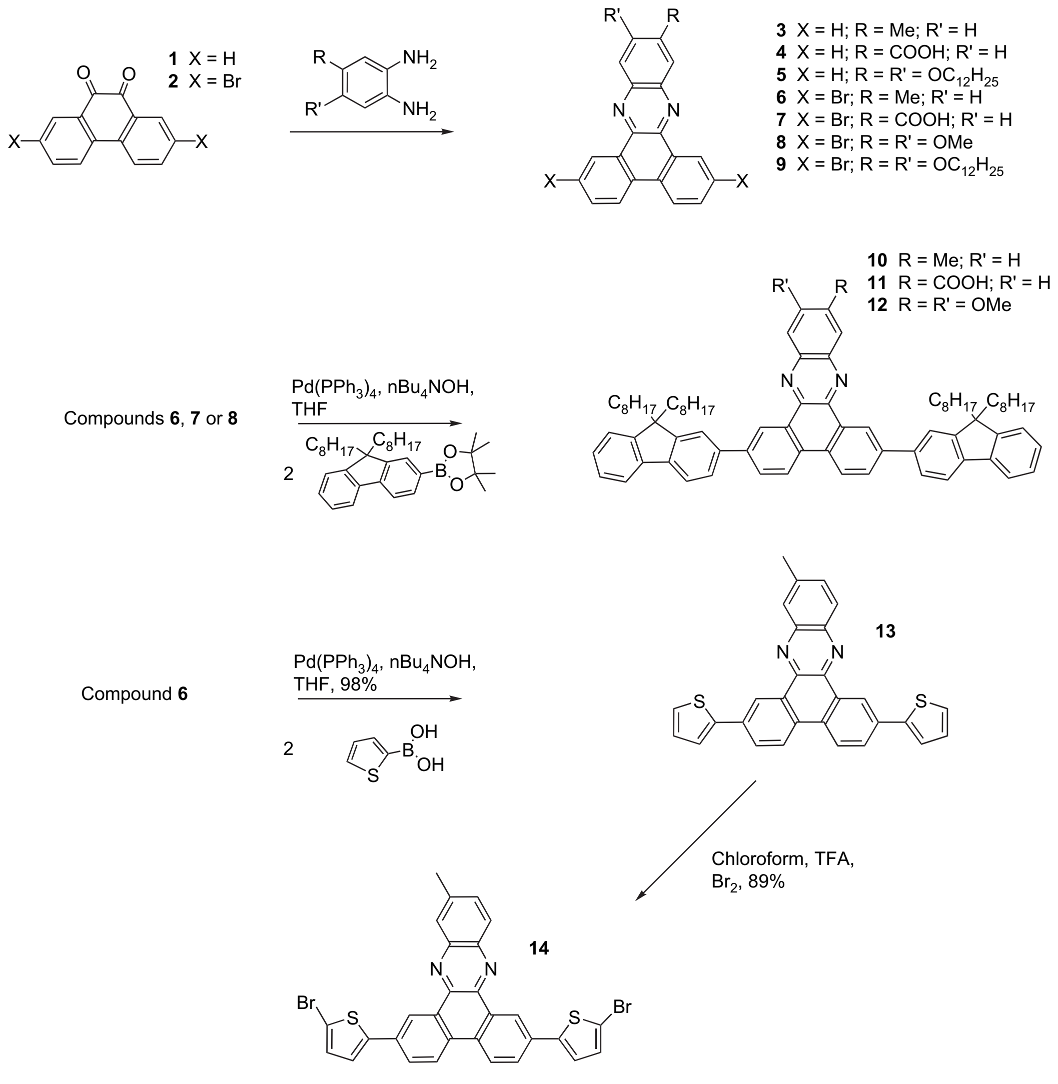

Scheme 1. Synthesis of the different model compounds.

N,*N*-dimethylformamide (DMF). In order to solve this problem, Yamamoto polymerisations of monomer **9** were carried out in toluene/DMF (10:3 v/v) solutions, using an Ni(COD)$_2$ catalyst. Under these reaction conditions high molecular weight polymer **23** (M_n, 36,400) was obtained and in high yield. Such a high molecular weight is typical of the Ni(COD)$_2$ catalyst system and is comparable to what can be found in the literature for other monomers [11].

The solubility properties in chloroform and THF of most of the synthetic materials were sufficient to allow structural characterisation to be carried out. Polymers **15**, **20** and **22**, however, only dissolved in chloroform/TFA mixtures (95/5 v/v), so it was not possible to carry out SEC analysis on these polymers.

The FT-IR spectra of all the model compounds and polymers display a band near 1605–1623 cm^{-1}, characteristic of C=N stretching modes, confirming the presence of phenazine moieties. Additionally, when alkyl or alkoxy substituents are present there are two bands between 3100 cm^{-1} and 2800 cm^{-1} corresponding to C–H aliphatic stretching modes. Finally, in the cases of compounds **4**, **7** and **11**, as well as polymer **18**, a very broad band between 3100 cm^{-1} and 2500 cm^{-1} and an intense band near 1689–1700 cm^{-1} are present. These correspond to the carboxylic acid O–H and C=O stretching modes, respectively.

The ^{1}H NMR spectra of model compounds **10–12** clearly show two sets of protons between 8.5 ppm and 9.8 ppm, which can be attributed to protons in the 1- and 4-positions. Such down-field protons are also present in the spectra obtained for the different polymers, with slight differences depending on the nature and number of substituents on the dibenzo[*a*,*c*]-phenazine moiety. Full assignment of the rest of the aromatic protons is more complex, due to the asymmetry of the compounds, and the large number of aromatic protons. However, various integrations, especially those between aromatic and aliphatic protons, are consistent with the expected structures. Interestingly, the ^{1}H NMR spectra of polymers **15**, **16**, **21** and **23** are very broad and featureless. This phenomenon could be due to aggregation of the polymer chains, which stiffens the structures and hinders their tumbling. As noted below, aggregation phenomena in chloroform solutions were further evidenced by SEC and, at sufficiently high concentrations, by gel formation.

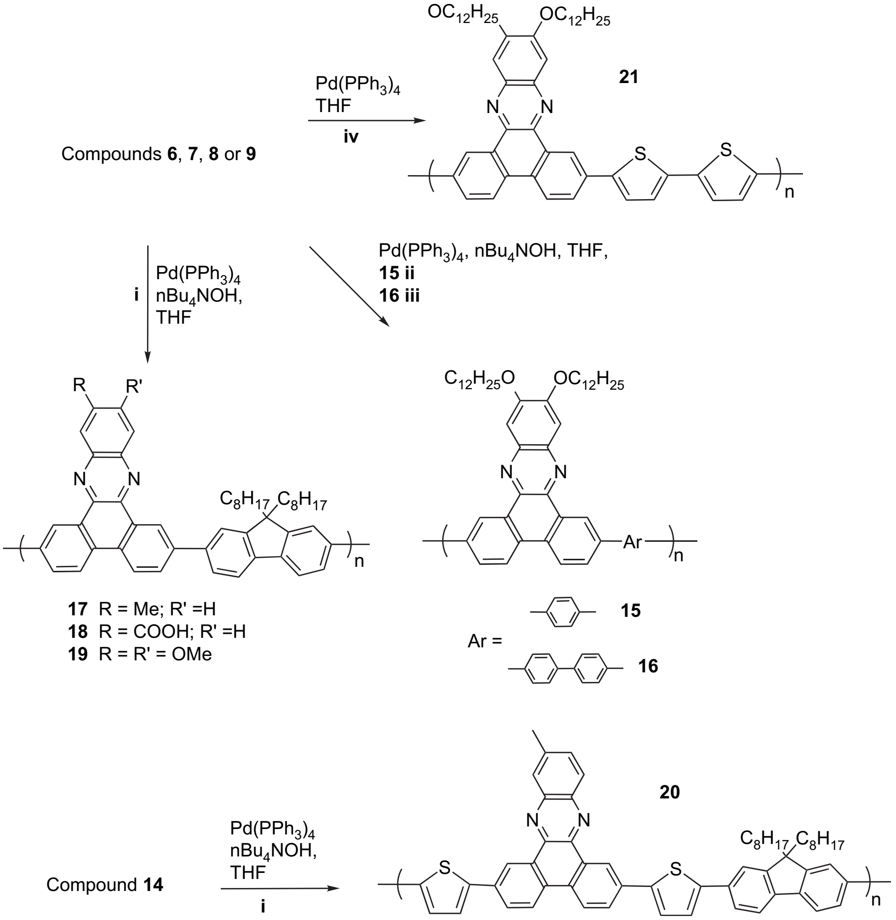

Scheme 2. Synthesis of co-polymers via Suzuki and Stille couplings. (i) 9,9-Dioctylfluorene-2,7-diboronic acid bispinacol ester; (ii) benzene-1,4-diboronic acid bispinacol ester; (iii) biphenyl-4,4′-diboronic acid bispinacol ester; (iv) bithienyl-5,5′-bis(tributylstannyl).

The ^{13}C NMR spectra of both the model compounds and the polymers show distinctive features, for example, the presence of signals at relatively high chemical shifts (between 140 ppm and 155 ppm) due to the quaternary carbons close to the nitrogen atoms of the dibenzo[*a*,*c*]phenazine moiety. The spectra recorded for compounds **4**, **7** and **11**, as well as for polymer **18**, display an additional peak near 170 ppm which can be attributed to the carbon of the carboxylic acid.

SEC results obtained, using polystyrene standards, for the different polymers are gathered in Table 1. For polymers **16**, **21** and **23**, SEC measurements were recorded in both THF and chloroform. Interestingly, in the latter solvent, the molecular weights were well beyond the calibration range of the polystyrene standards (220–1,800,000), while in THF the molecular weights (M_n) fall between 18,800 and 36,400. This indicates that a strong aggregation phenomenon occurs in chloroform solutions even at the low concentrations used for the SEC analyses (0.5 mg mL^{-1}).

Finally, polymers **15** and **22** were too insoluble in chloroform or THF for SEC analysis, so MALDI-TOF-MS were recorded to assess their molecular weights. Oligomers up to the hexamer, in the case of **22**, and up to the tetramer, in the

Table 1
Results obtained for the polymerisation of various dibenzo[*a*,*c*]phenazine-based monomers

Polymer	Catalyst	Yield (%)	M_w[a]	M_n[a]	MWD[a]	Solubility in THF
15	$Pd(PPh_3)_4$	99	NA	NA	NA	Partially soluble
16	$Pd(PPh_3)_4$	55	32,200	24,700	1.30	Soluble
17	$Pd(PPh_3)_4$	65	8200	3800	2.16	Soluble
18	$Pd(PPh_3)_4$	93	3500	2400	1.04	Soluble
19	$Pd(PPh_3)_4$	91	10,900	5500	1.98	Soluble
20	$Pd(PPh_3)_4$	88	NA	NA	NA	Insoluble
21	$Pd(PPh_3)_4$	74	26,600	18,800	1.41	Soluble
22	$NiCl_2$	75	NA	NA	NA	Insoluble
23	$Ni(COD)_2$	99	68,800	36,400	1.89	Soluble

[a] Determined by SEC analysis, relative to polystyrene standards. NA: not available.

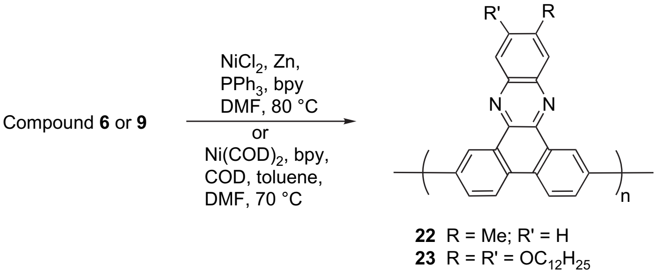

Scheme 3. Synthesis of homopolymers via Yamamoto coupling.

case of **15**, were observed with increments of 292 g mol^{-1} and 723 g mol^{-1}, respectively, consistent with the expected structure of the repeat units. The nature of the end-groups could not be determined in the case of **22**, but bromine and hydrogen atoms are likely candidates. In the case of **15**, the oligomers were found to be hydrogen capped, with terminal phenyl or dibenzo[*a*,*c*]phenazine moieties.

3.2. UV–vis and fluorescence spectroscopies

The spectroscopy of many phenazine derivatives has been studied and the photophysical processes taking place in these compounds have been shown to depend greatly on the nature of their substituents [12]. Phenazine itself possesses a low-lying n–π* singlet state, approximately 0.2 eV below its first π–π* singlet state (which is itself 2.8 eV above the ground state), as well as a π–π* triplet state situated 1.8 eV above the ground state [12]. This arrangement of energy levels explains why phenazine is only very weakly fluorescent ($\varphi_{\text{fl}} \approx 3.10^{-5}$) yet, due to strong intersystem crossing between the first n–π* singlet state and the first π–π* triplet state ($\varphi_{\text{isc}} \approx 0.98$), strongly phosphorescent [13]. Dibenzo[*a*,*c*]phenazine derivatives have received far less attention, but they have been shown to possess a low-lying π–π* singlet state, with the n–π* singlet state situated slightly above (although its exact position was not determined) [14]. Such a configuration explains the increased fluorescence of dibenzo[*a*,*c*]phenazines, compared to phenazine.

In the present project, the UV–vis and fluorescence spectra of the model compounds were studied first. Model compounds **3** and **5** are soluble in various organic solvents. Their UV–vis and fluorescence spectra were recorded in chloroform (see Fig. 2). Both compounds display similar spectra with a relatively sharp highest transition at *ca.* 400 nm. The small red shift observed for this transition when going from compound **3** to compound **5** can presumably be attributed to the alkoxy substituents. This absorption band seems to have a π–π* nature, as evidenced by its small shift when varying the polarity and dielectric constant of the solvent (see Supporting information) and its high extinction coefficient [15]. The fluorescence spectra of compounds **3** and **5** give further support for the π–π* nature of the highest transition. Both compounds fluoresce in the blue region and have small Stokes' shifts (6 nm and 11 nm, respectively). Interestingly, the quantum yields calculated for compounds **3** and **5** are 0.9% and 82%, respectively. This enhancement of the fluorescence quantum yield for the dialkoxy derivative is believed to be due to a stabilisation of the π–π* state, making the gap between this state and the higher n–π* state larger. In the solid state, the fluorescence λ_{max} of compound **5** is red-shifted by 36 nm, compared to the solution λ_{max}. Such an effect is a good indication that aggregation occurs for such dialkoxy derivatives and provides further evidence that aggregation phenomena are indeed observed by SEC and ^{1}H NMR for the didodecyloxydibenzo[*a*,*c*]phenazine-based polymers.

The UV–vis and fluorescence spectroscopies of the model compounds **10–12**, containing two dioctylfluorene moieties, were studied next. These are significantly different from their 2,7-unsubstituted parents: see Fig. 3. The π–π* transition that is present near 400–415 nm in the UV–vis spectra of compounds **3** and **5** is still present in those of derivatives **10–12**. However, an additional broad band near 340 nm, presumably due to the conjugated backbone of the molecule, is observed. Also, a broad and relatively weak band is observed for models **10** and **11** above 410 nm. This band could be due to an intramolecular charge transfer (CT) phenomenon between the dioctylfluorene and the dibenzo[*a*,*c*]phenazine moieties, similarly to what was recently reported by Jenekhe and co-workers for

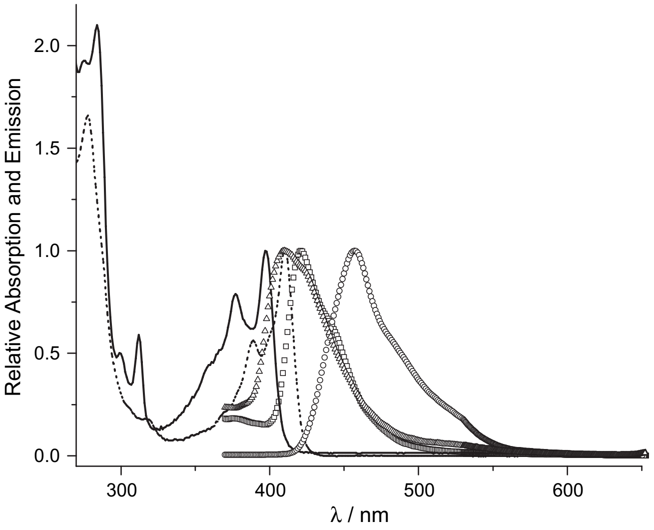

Fig. 2. UV–vis and fluorescence spectra of compounds **3** and **5**. Absorption spectra were recorded in chloroform (solid line, **3** and dotted line, **5**) and emission spectra were recorded in chloroform (triangles, **3** and squares, **5**) as well as in the solid state (circles, spin coated film of **5**); $\lambda_{\text{excitation}}$: 398 nm (**3**) and 409 nm (**5**).

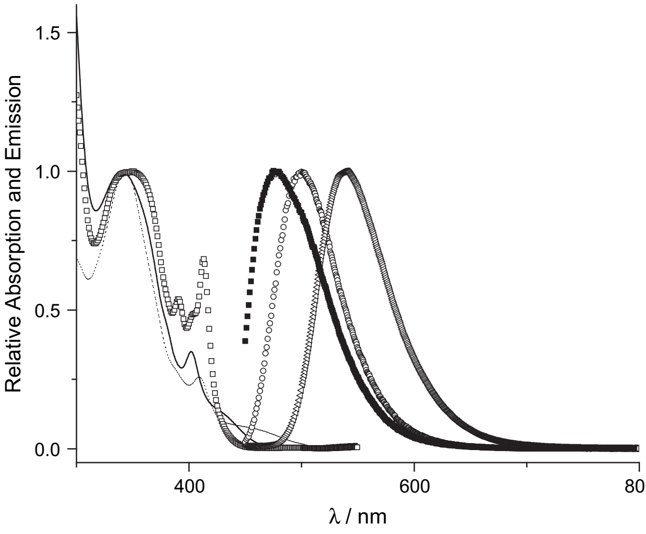

Fig. 3. UV–vis (**10**, solid line; **12**, dotted line; **11**, open squares) and emission (**10**, circles; **12**, filled squares; **11**, triangles) spectra of 2,7-bis(dioctylfluorene)dibenzo[*a*,*c*]phenazine derivatives, spin coated on quartz slides; $\lambda_{\text{excitation}}$: 400 nm.

poly(dibenzo[*a*,*c*]phenazine-3,6-diyl-*co*-9′,9′-dioctylfluorene-2′,7′-diyl) [7d]. The fact that this highest transition is very sensitive to the nature of the substituents at the 11- and 12-positions is further evidence of the CT character of this band. Thus, for compound **11**, the dibenzo[*a*,*c*]phenazine moiety is more electron-deficient and the band is more red-shifted; for compound **10**, the dibenzo[*a*,*c*]phenazine is slightly more electron-rich, therefore the red shift of the band is slightly smaller and overlaps with the $\pi-\pi^*$; for compound **12**, the dibenzo[*a*,*c*]phenazine is even more electron-rich and the CT band is hidden by the $\pi-\pi^*$ transition. The fluorescence spectra of compounds **10–12** follow a similar trend: the more red-shifted the CT band in the UV–vis spectra, the higher the λ_{max} of emission. Moreover, the Stokes' shifts observed for compounds **10–12** are of the order of 100 nm (in the blue-green region), which is typical in the case of CT transitions.

Attention was then turned to the UV–vis and fluorescence spectra of the polymers. If polymers of the present types were to be used in electronic devices, they would almost certainly be present as thin films. Accordingly their spectra in this state are of particular interest. Of the polymers discussed in the present project the soluble ones with relatively high molecular weights, i.e. polymers **16**, **21** and **23** are of greatest interest. Polymers **16**, **21** and **23** were sufficiently soluble in THF and chloroform that they can be cast easily as uniform transparent films. In addition, it was possible to cast homogenous films of polymer **15** from chloroform/TFA 95/5 mixtures. TFA was fully removed from the film by extensive drying in vacuum, as was evidenced by colour change. Fig. 4a shows the UV–vis spectra obtained for thin films of polymers **15**, **16**, **21** and **23**. As with the bis(dioctylfluorene)-containing model compounds **10–12**, a band appears near 350 nm for polymers **15** and **16** and is red-shifted to 370 nm for polymer **23**. It is even more red-shifted for polymer **21**, although the breadth of the band overlaps with other transitions and so does not allow precise determination of its position. Such a trend in the evolution of this peak is probably due to the gradual decrease of the overall twist in the polymer backbone in the order of polymer **16** > **15** > **23** > **21**, which causes an increase of the conjugation length. All four UV–vis spectra display a band near 410 nm that is reminiscent of the highest transition observed for compound **5**. This band is the highest transition for polymers **15**, **16** and **23**, although a small tail at higher wavelength could indicate the presence of weak CT transitions, similarly observed for the dioctylfluorene-containing model compounds. Polymer **21** also clearly displays additional bands between 410 nm and 550 nm which may be attributed to CT phenomena.

The fluorescence spectra obtained for thin films of polymers **15**, **16**, **21** and **23** are shown in Fig. 4b. The emission spans the blue-green to red region with λ_{max} falling between 490 nm, for polymer **15**, and 590 nm for polymer **21**. The higher λ_{max} observed for this latter polymer can easily be rationalized as arising from the higher onset of UV–vis absorption. The situation for other polymers is more difficult to fully understand. Two phenomena are presumably taking place: CT phenomena, similar to those observed for bis(dioctylfluorene)-containing model compounds, and aggregation phenomena, similar to those observed for compound **5**. Aggregation seems to be more pronounced in the case of polymer **23**, for which a large shift in emission λ_{max} is observed when drop casting, as opposed to spin coating, is used to deposit the polymer onto glass slides.

Because of the low solubility of polymers **22** and **17** and the poor quality of the films that they formed, their UV–vis spectra were recorded in chloroform/TFA (95:5 v/v) solutions (see Supporting information). The increase of the conjugation length along the polymer backbone when going from compound **3** to polymer **22** to polymer **17** translates as a red shift of a transition from 320 nm to 380 nm (**3** and **17**, respectively). A broad absorption peak present at longer wavelength (with the onset of absorption ranging from 500 nm to 700 nm) which

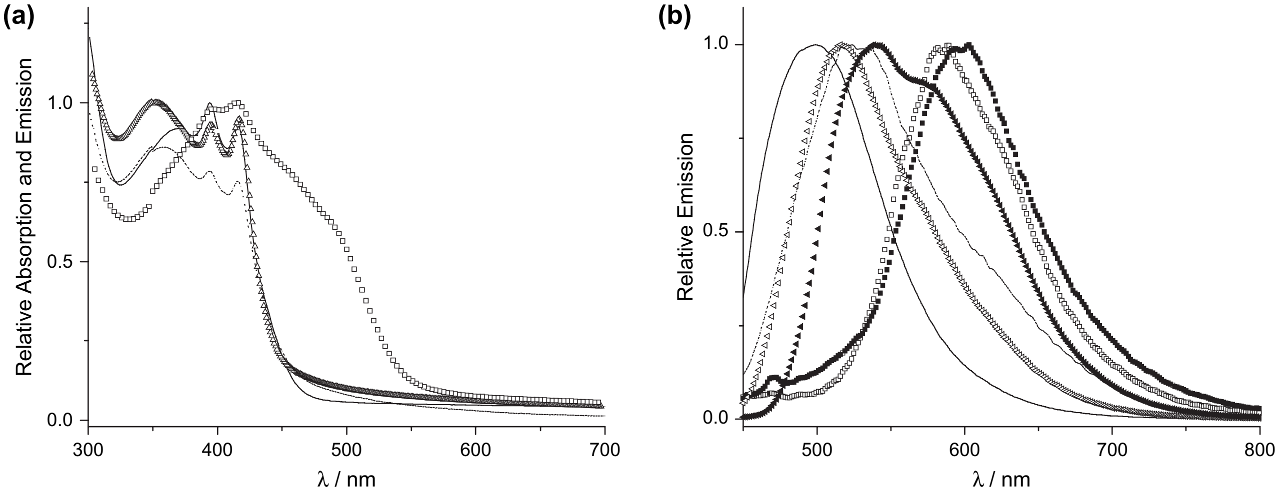

Fig. 4. UV–vis and fluorescence spectra of various dibenz[*a*,*c*]phenazine-based polymer films. (a) Absorption spectra of spin coated films of polymers **15** (dotted line), **16** (triangles) **21** (open squares) and **23** (solid line); (b) emission spectra of spin coated films of polymers **15** (dotted line), **16** (solid line), **21** (open squares) and **23** (open triangle), and drop cast films of polymers **21** (filled squares) and **23** (filled triangles); $\lambda_{excitation}$: 400 nm.

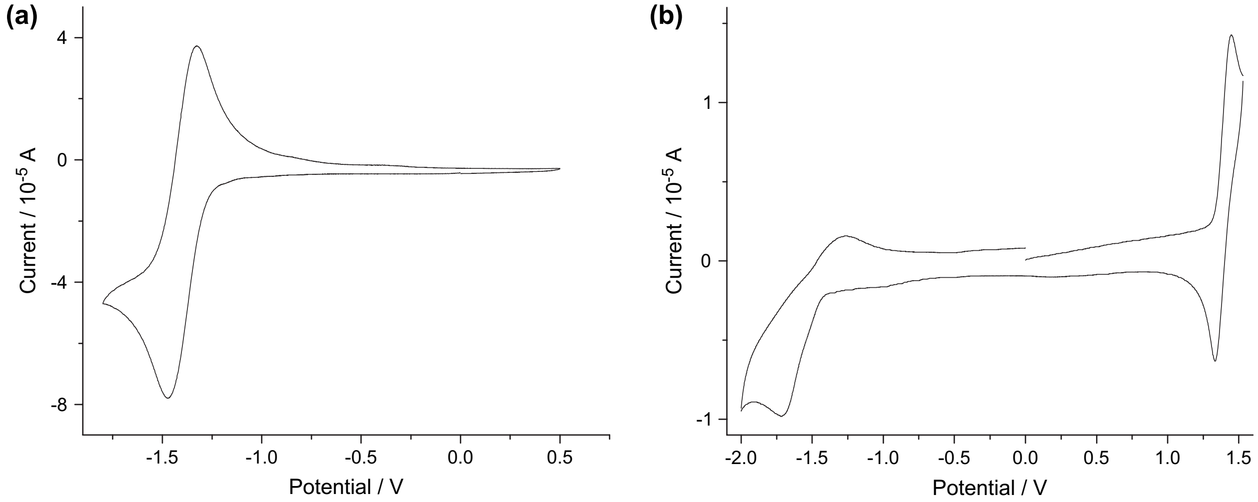

Fig. 5. Cyclic voltammograms of compounds **3** (a) and **12** (b) in $TBAPF_6$ (0.1 mol L^{-1}) solutions in degassed anhydrous DCM (3 mmol L^{-1}, scan rate: 0.1 V s^{-1}), vs Ag/AgCl.

is absent in the spectrum of **3** recorded in pure chloroform is presumably due to protonation of the dibenzo[*a*,*c*]phenazine moieties. Under these conditions, no fluorescence was observed for any of these materials. Indeed the N–H bonds formed by protonation of the dibenzo[*a*,*c*]phenazine moieties provides a pathway for non-radiative decays and fluorescence is quenched [15].

3.3. Cyclic voltammetry

The cyclic voltammograms obtained for model compounds **3** and **5** both display a single reversible reduction peak with a half-wave potential of −1.40 V and −1.47 V (vs Ag/AgCl), respectively. Fig. 5a shows a typical voltammogram. Phenazine itself displays two reduction potentials in acidic conditions ($HClO_4$ or HCl solutions) [7c,16], corresponding to two successive one-electron transfers. The presence of only one reduction potential in the voltammograms of **3** and **5** could be interpreted as the occurrence of one single two-electron transfer or could be due to a much more negative potential for the second reduction step. No conclusive evidence is available for deciding between these two scenarios. However, the more negative half-wave potential observed for compound **5** can easily be rationalized, according to the Hammett theory, since the alkoxy substituents have a more negative σ_p constant than the methyl group.

The cyclic voltammograms obtained for bis(dioctylfluorene)-containing compounds **10–12** have significantly different shapes compared to those obtained for 2,7-substituted dibenzo[*a*,*c*]phenazines: see Fig. 5b. Similar asymmetric shapes for the reduction peak were reported for phenazine-based polymers (in cases where electrochemical measurements were recorded using neutral aqueous or acetonitrile solutions) and were not associated with irreversibility [7a,c]. Upon reduction, processes such as charge transfer and structural reorientation are likely to take place within this family of compounds and could account for the asymmetry of the reduction peak. Again, the position of the reduction peak is easier to rationalize and seems to be set by the nature of the substituents

Table 2
Electrochemical results obtained for dibenzo[*a*,*c*]phenazine derivatives **3**, **5** and **10–12**

Model	$1/2(E_{pa}+E_{pc})$[a] (mV)	ΔE[a] (mV)	$1/2(E_{pa}+E_{pc})$[b] (mV)	ΔE[b] (mV)	E(ox) − E(red) (mV)
3	−1400	140	None	None	NA
5	−1470	140	None	None	NA
10	−1410	480	1450	190	2860
11	−1350	300	1490	130	2840
12	−1450	480	1390	110	2840

Results obtained in degassed anhydrous DCM solutions (electrolyte: $TBAPF_6$, 0.1 mol L^{-1}; scan rate: 0.1 V s^{-1}), vs Ag/AgCl.

[a] Reduction.

[b] Oxidation.

Table 3
Electrochemical results obtained for the different polymer films

Polymer	$1/2(E_{pa}+E_{pc})$ (mV)	ΔE (mV)	Electron affinity[c] (eV)	$1/2(E_{pa}+E_{pc})$[a] (mV)	ΔE[a] (mV)
15	−2310	Irreversible	2.7	NA	NA
16	−2360	Irreversible	2.6	−1420	140
17	−1420	300	3.1	NA	NA
18	−1720	270	2.8	NA	NA
19	−1450	200	3.1	NA	NA
20	−2200	Irreversible	2.7	NA	NA
21	−2210	Irreversible	2.7	−1340	140
22	−1400	150	3.2	NA	NA
23	−1660	1340	2.8	−1200	[b]

Films coated on glassy carbon electrodes using degassed acetonitrile (electrolyte: $TBAPF_6$, 0.1 mol L^{-1}; scan rate: 0.1 V s^{-1}), vs Ag/AgCl.

[a] Results obtained for 3 mmol L^{-1} degassed anhydrous THF polymer solutions, with $TBAPF_6$ (0.1 mol L^{-1}) electrolyte (scan rate: 0.1 V s^{-1}), vs Ag/AgCl.

[b] The resolution of the peak is insufficient to determine the exact position of the peak.

[c] Electron affinities were calculated from the onset potentials for reduction E_{on}(red), using the equation: $EA = 4.4 + E_{on}(red)$ [18].

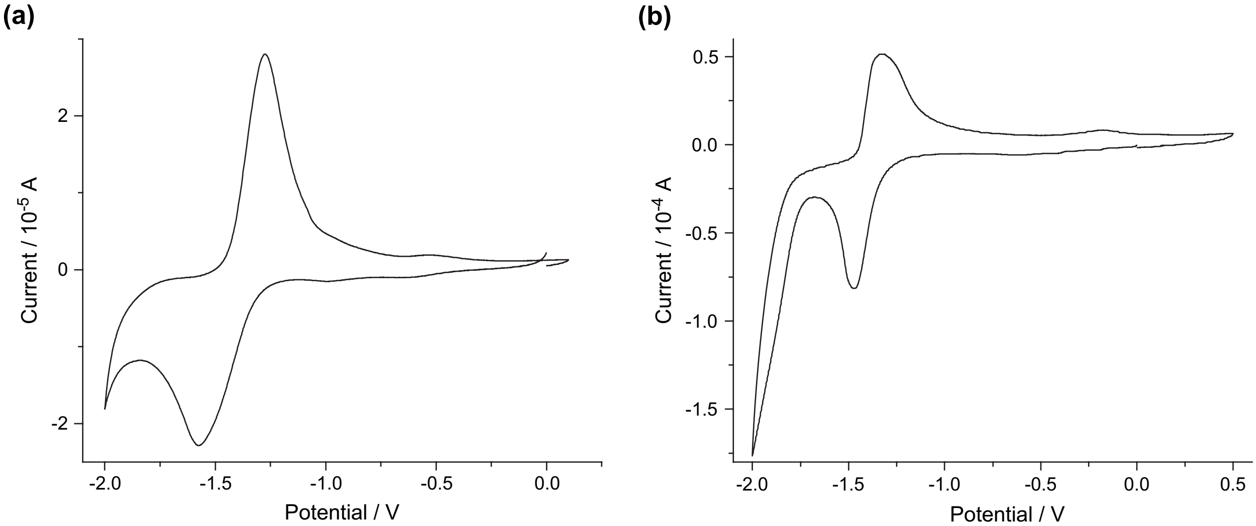

Fig. 6. Cyclic voltammograms of polymers **17** (a) and **22** (b) films on glassy carbon electrode in TEAPF$_6$ (0.1 mol L^{-1}) solution in degassed acetonitrile (scan rate: 0.1 V s^{-1}), vs Ag/AgCl.

in the 11- and 12-positions: electron-donor substituents shift the half-wave potential to more negative values, while electron-acceptor substituents shift it to more positive ones (Table 2). Finally, a reversible oxidation process can be observed on the cyclic voltammograms of derivatives **10–12**. This process takes place near 1.4 V and its exact position also seems to be determined by the nature of the substituents in the 11- and 12-positions. This means that the electrochemical gap between HOMO and LUMO are almost identical for derivatives **10–12**, but the positions of both levels can be tuned by changing the nature of the substituents in the 11- and 12-positions. This effect could have important implications for fine tuning the properties of the materials for device optimisation.

The electrochemical results obtained for the different polymer films are gathered in Table 3. Examples of cyclic voltammograms are displayed in Fig. 6. The results obtained for polymers **17–19** and **22** follow a similar trend to that of model compounds **10–12**, except for polymer **18** which displays a half-wave potential cathodically shifted. The asymmetry of the peaks observed is likely to be due to various phenomena, such as solvation of the reduced polymer chains, modification of the diffusion patterns, aggregation and "break in" effects [17]. In the case of didodecyloxydibenzo[*a*,*c*]phenazine-based polymers **15**, **16**, **20**, **21** and **23**, highly asymmetric peaks were observed, to the extent that no reoxidation was detected for copolymers **15**, **16** and **21**. In THF solutions, however, quasi-reversible peaks are observed near −1.4 V, which is similar to that observed for the different model compounds. This could indicate that reduction processes do not take place or are hindered in the solid state. Full investigation of this phenomenon still remains to be carried out. Finally, the electron affinities of the different polymers were calculated from the onset potentials for reduction, following a method reported in the literature [18], and were found to fall between 2.6 eV and 3.2 eV.

4. Conclusions

The synthesis of a novel family of electron-accepting conjugated polymers based on dibenzo[*a*,*c*]phenazine has been developed. The structures of the different materials were confirmed using NMR and IR spectroscopies and, in some cases, mass spectrometry. Many polymers had poor solubilities but polymers **16**, **21** and **23**, containing two dodecyl groups in the 11- and 12-positions of the dibenzophenazine units, are quite soluble in chloroform and THF. These polymers were obtained with molecular weights (M_n) in the range 18,800–36,400. The photophysical as well as electrochemical properties of the different model compounds and the polymers were found to be quite sensitive to the substituents in the 11- and 12-positions of the dibenzophenazine units. The materials emit light in the green to orange region. Moreover, the didodecyloxydibenzo[*a*,*c*]phenazine derivatives display aggregation properties. This is an interesting feature where electron transport is concerned. The properties of the soluble polymers suggest that others of a similar type could find applications in microelectronics and are, therefore, worthy of further study.

Acknowledgements

We thank Valerie Boote for performing the MALDI-TOF-MS measurements, Dr. Abderazzack Ben Haida for the synthesis of the diaminodialkoxybenzenes, Professor Peter Skabara for his help with the CV measurements and Professor Stephen Faulkner for his help with the fluorescence measurements.

Appendix. Supporting information

UV–vis spectra of **5** in different solvents, UV–vis spectra of **3**, **17** and **22** in chloroform/TFA (95/5 v/v mixtures) and cyclic voltammograms of **5**, **10**, **11**, **15**, **16**, **18–21** and **23**. Supplementary data associated with this article can be found, in the online version, at doi:10.1016/j.polymer.2007.09.045.

References

[1] (a) Dimitrakopoulos CD, Mascaro DJ. IBM J Res Dev 2001;45:11–27;
(b) Karl N. Synth Met 2003;133–134:649–57;
(c) Paasch G, Lindner T, Scheinert S. Synth Met 2002;132:97–104;
(d) Baughman RH, Bredas J-L, Chance RR, Elsenbaumer RL, Shacklette LW. Chem Rev 1982;82:209–22.

[2] (a) Bredas J-L, Calbert JP, da Silva Filho DA, Cornil J. Proc Natl Acad Sci USA 2002;99:5804–9;
(b) Gruhn NE, da Silva Filho DA, Bill TG, Malagoli M, Coropceanu V, Kahn A, et al. J Am Chem Soc 2002;124:7918–9;
(c) Kwon O, Coropceanu V, Gruhn NE, Durivage JC, Laquindanum JG, Katz HE, et al. J Chem Phys 2004;120:8186–94;
(d) Lemaur V, da Silva Filho DA, Coropceanu V, Lehmann M, Geerts Y, Piris J, et al. J Am Chem Soc 2004;126:3271–9.

[3] (a) Sirringhaus H, Brown PJ, Friend RH, Nielsen MM, Bechgaard K, Langeveld-Voss BMW, et al. Nature 1999;401:685–8;
(b) Ong BS, Wu Y, Liu P, Gardner S. J Am Chem Soc 2004;126:3378–9.

[4] Chua L-L, Zaumseil J, Chang J-F, Ou EC-W, Ho PK-H, Sirringhaus H, et al. Nature 2005;434:194–9.

[5] (a) Chen XL, Jenekhe SA. Macromolecules 1997;30:1728–33;
(b) Arnold FE, Van Deusen RL. Macromolecules 1969;2:497–502.

[6] Crispin X, Cornil J, Friedlein R, Okudaira KK, Lemaur V, Crispin A, et al. J Am Chem Soc 2004;126:11889–99.

[7] (a) Yamamoto T, Okuda T. J Electroanal Chem 1999;460:242–4;
(b) Izumi A, Nomura R, Masuda T. Macromolecules 2000;33:8918–20;
(c) Puskas Z, Inzelt G. Electrochim Acta 2005;50:1481–90;
(d) Zhu Y, Gibbons KM, Kulkarni AP, Jenekhe SA. Macromolecules 2007;40:804–13.

[8] (a) Coulson DR. Inorg Synth 1972;8:121;
(b) Adapted from: Belletete M, Beaupre S, Bouchard J, Blondin P, Leclerc M, Durocher G. J Phys Chem B 2000;104:9118–25;
(c) Wei Y, Yang Y, Yeh J-M. Chem Mater 1996;8:2659–66;
(d) Schmidt J, Junghans E. Chem Ber 1904;37:3558;
(e) Kantekin H, Ocak U, Gok Y, Alp H. Polyhedron 2002;21:1865–70.

[9] (a) Demas JN, Crosby GA. J Phys Chem 1971;75:991–1024;
(b) Iraqi A, Wataru I. Chem Mater 2004;16:442–8.

[10] (a) Roberts RM, Browder HP, Kobe KA. J Am Chem Soc 1959;81:1165–7;
(b) Musante C, Fabbrini L. Sper Sez Chim Biol 1952;3:33–44.

[11] (a) Kwiatkwoski GT, Matzner M, Colon I. Pure Appl Chem 1997;34:1945–75;
(b) Yamamoto T, Muramatsu Y, Lee B-L, Kokubo H, Sasaki S, Hasegawa M, et al. Chem Mater 2003;15:4384–93;
(c) Yamamoto T, Etori H. Macromolecules 1995;28:3371–9.

[12] (a) Badger GM, Walker IS. J Chem Soc 1956:122–6;
(b) Hochstrasser RM. J Chem Phys 1962;36:1808–13.

[13] (a) Hirata Y, Tanaka I. Chem Phys Lett 1976;43:568–70;
(b) Carvalho CEM, Brinn IM, Pinto AV, Pinto MDCFR. J Photochem Photobiol A Chem 2000;136:25–33;
(c) Nickel B, Ruth AA. J Phys Chem 1991;95:2027–36.

[14] (a) Davis GA. Tetrahedron Lett 1971;12:3045–8;
(b) Guha SK, Banerji KD, Sen KK. J Indian Chem Soc 1972;49:815–8.

[15] Turro NJ. Modern molecular photochemistry. Reading, MA: Addison-Wesley Publishing Co.; 1991.

[16] Paduszek B, Kalinowski MK. Electrochim Acta 1983;28:639–42.

[17] Iraqi A, Crayston JA, Walton JC. J Mater Chem 1998;8:31–6.

[18] (a) Janietz S, Barche J, Wedel A, Sainova D. Macromol Chem Phys 2004;205:187–98;
(b) Janietz S, Bradley DDC, Grell M, Giebeler C, Inbasekaran M, Woo EP. Appl Phys Lett 1998;73:2453–5.